Biotypes of deeply phenotyped depressed patients reflect signatures of adverse childhood experience and depressive cognitive biases

Federica Colombo[1*], Federico Calesella[1,6], Beatrice Bravi[1], Lidia Fortaner-Uyà[1,2], Camilla Monopoli[1], Tommaso Cazzella[1,2], Michele Acconcia[1,7], Raffaella Zanardi[2,3], Cristina Colombo[2,3], Matteo Carminati[1], Chiara Fabbri[4], Alessandro Serretti[5], Irene Bollettini[1], Francesco Benedetti[1,2], Sara Poletti[1,2], Benedetta Vai[1,2]

1 Psychiatry and Clinical Psychobiology Unit, Division of Neuroscience, IRCCS Ospedale San Raffaele, Milano, Italy

2 Università Vita-Salute San Raffaele, Milano, Italy

3 IRCCS Ospedale San Raffaele, Mood Disorders Unit, Milano, Italy

4 University of Bologna, Department of Biomedical and Neuromotor Sciences, Bologna, Italy

5 Department of Medicine and Surgery, Kore University of Enna, Enna, Italy

6 Present address: Padova Neuroscience Center, University of Padova, Padova, Italy

7 Present address: Functional Neuroimaging Laboratory, Center for Neuroscience and Cognitive Systems, Istituto Italiano di Tecnologia, Rovereto, Italy

***Corresponding author:** Federica Colombo (colombo.federica@hsr.it)

Sara Poletti and Benedetta Vai are co-senior authors.

Abstract

Background: Negative Cognitive Styles (NCS) are key features of depression contributing to severe clinical outcomes by sustaining negative affect. However, depression is clinically heterogeneous, reflecting complex neurobiological and environmental interactions. Characterizing heterogeneity using multimodal data could help identify mechanisms mapping onto different phenotypes and discover high-impact biomarkers.

Methods: Using a stability-based relative clustering validation pipeline, 344 depressed patients (135 major depressive disorder, 209 bipolar disorder) were stratified based on multimodal neuroimaging data, including grey matter volumes, cortical thickness, white matter diffusivity indices, resting-state functional connectivity (FC), and spontaneous neural activity. Clusters were derived from each modality separately and in combination, and profiled for Adverse Childhood Experiences (ACEs) and NCS.

Results: All neuroimaging modalities stratified depressed patients into two clusters, with the FC-based model achieving the highest accuracy (85%). Compared with healthy controls (HC, N=138), these clusters exhibited opposite patterns of global functional hyper-integration (Cluster 1) and hyper-segregation (Cluster 2). Unique multivariate neurobiological-ACEs relationships characterized the FC-based clusters. While ACEs negatively affected FC in Cluster 1 and HC, Cluster 2 showed opposite effects specific to ACE subtypes, with sexual abuse positively influencing FC. Mediation analysis showed that FC strength mediated the relationship between ACEs and NCS of overgeneralize only in Cluster 2. ACE-related functional alterations pinpoint brain regions involved in socioemotional and cognitive development, sensitive to maturational neural changes. **Conclusions:** These findings provide evidence of clinically meaningful depression "biotypes" shaped by ACEs and associated with NCS, underlining the feasibility of computational psychiatry tools to uncover data-driven patterns for precision psychiatry.

Keywords: Depression, Adverse Childhood Experience, Cognitive Biases, Machine Learning, Neuroimaging, Biotypes

Introduction

Depressive disorders carry a substantial social and economic burden, demanding more personalized and effective clinical strategies (Cirone et al., 2021; GBD Mental Disorders Collaborators, 2022). Negative Cognitive Styles (NCS) - including dysfunctional attributional styles and negative thinking – are key prognostic factors in the onset and maintenance of depression (Beck, 2008). NCS are associated with poor therapeutic responses and increased suicidality (Fazakas-DeHoog et al., 2017; Shankman et al., 2013; Zhou et al., 2021), while targeted interventions can improve clinical symptoms and overall functioning (Jones and Sharpe, 2017; Scheepens et al., 2022; Spinhoven et al., 2018). Identifying the factors that influence and moderate NCS is of critical importance, particularly given the substantial heterogeneity in how patients may respond to treatments (Maslej et al., 2021).

It is widely recognised that environmental factors significantly contribute to the variance associated with mood disorders, and, by interacting with genetic predisposition, determine their clinical manifestation (Kendall et al., 2021). Adverse Childhood Experiences (ACEs), such as abuse and neglect, represents a key risk factor for psychopathology, including depression (McLaughlin et al., 2020; Poletti, Colombo, et al., 2014; Wade et al., 2022). Individuals exposed to ACEs often experience a worse illness course, including poor treatment response and increased suicidality (Blair et al., 2025; Giampetruzzi et al., 2023; Hayashi et al., 2015). Cognitive theories of depression propose that ACEs foster NCS by shaping early maladaptive cognitive patterns (Beck, 2008). This pathway could be potentially driven by ACEs-related structural and functional brain alterations (Teicher and Samson, 2013), which primarily impact networks governing emotion regulation, threat detection, and cognitive functions (Teicher et al., 2016; Yan et al., 2025). Exposure to ACEs was indeed shown to affect neural correlates specifically associated with psychiatric conditions, including grey matter (GM) volumetric reductions and white matter (WM) disruption (Benedetti et al., 2011, 2012, 2014; Poletti et al., 2014b, 2016, 2018), and associates with worse outcomes and higher suicidality (Vai, Serretti, et al., 2020).

Understanding how these factors moderate and predict clinical outcomes is a primary objective of precision psychiatry, where the identification of patient-specific characteristics enables the optimal prediction of intervention efficacy (Bzdok and Meyer-Lindenberg, 2018; Fernandes et al., 2017; Tiego et al., 2023). However, these interactions are unlikely to be consistent across patients, reflecting transdiagnostic heterogeneity (Xie et al., 2023). Recent research has identified neurobiological subtypes (i.e., biotypes) of depression, offering a data-driven stratification to better capture clinical and biological diversity. For instance, increased default mode network functional connectivity (FC) was linked to a “rumination” biotype (Goldstein-Piekarski et al., 2022; Williams, 2017, 2016), while heightened activity within the cognitive control circuit predicts negative biases and treatment response (Tozzi et al., 2024). Nevertheless, stratification studies have predominantly relied on resting-state functional MRI (Drysdale et al., 2017; Liang et al., 2020; Price et al., 2017; Tokuda et al., 2018), leaving the structural basis largely unexplored. We recently identified distinct biotypes of major depressive disorder (MDD) using structural neuroimaging: one marked by reduced GM, cortical thickness (CT), and WM integrity - linked to anergy, childhood abuse, and

inflammatory markers - and another with more preserved structure, associated with cognitive symptoms (e.g., negative self-esteem) (Colombo et al., 2024). However, exploring interactions between ACEs and NCS in different biotypes for multimodal neuroimaging data remain unaddressed.

In this study we aimed to address these gaps by providing a unique neuroimaging-driven stratification through an unsupervised machine learning (ML) approach in depressed MDD and bipolar disorder (BD) patients, using multimodal structural and functional brain imaging data. We then examined the neurobiological and clinical features of each cluster, focusing on the relationships between NCS, ACEs, and neural correlates. Finally, we explored whether ACEs-related brain signatures mediates the relationship between ACEs and NCS using multivariate models, which are well-suited to capture complex brain-behavior associations underlying psychiatric heterogeneity (Sha et al., 2019; Xie et al., 2023).

Methods and Materials

Participants

The sample included 344 inpatients (135 MDD, 209 BD), consecutively admitted at the IRCCS San Raffaele Hospital (Milan, Italy) and diagnosed according DSM-5 criteria using the Structured Clinical Interview for the Diagnosis of Axis I Disorders (SCID-5). Inclusion criteria were age 18-65 years old and current depressive episode. Depression severity was assessed with the 21-items Hamilton Depression Rating Scale (HDRS-21) (Hamilton, 1986). Exclusion criteria for all patients included: major medical and neurological disorders, pregnancy, intellectual disability, history of drug or alcohol abuse or dependency, and psychiatric comorbidity on axis I. A sample of 138 healthy controls (HC) without psychiatric history or first-degree familial risk was also recruited. MRI acquisitions were performed for all participants between 2.30 pm and 6.00 pm. After a complete description of the study, written informed consent was obtained. All procedures contributing to this work comply with the ethical standards of the relevant national and institutional committees on human experimentation and with the Helsinki Declaration of 1975, as revised in 2008. The study was approved by the local ethical committee.

Sociodemographic, childhood trauma and cognitive styles measures

Age, sex, number of previous mood episodes, age of onset, duration of illness, and years of education were collected. Medication load was calculated for each subject categorizing each medication into 0-4 scores based on dose range, and then combined to obtain a single composite score (see **Methods S1** for detailed criteria) (Sackeim, 2001). In a subsample of 229 patients (106 MDD, 123 BD) and 98 HC, childhood trauma was assessed through the 28-item version of the Childhood Trauma Questionnaire (CTQ) (Bernstein et al., 2003), which investigates 5 categories of childhood trauma: physical, emotional, and sexual abuse; physical and emotional neglect. Each form of maltreatment is evaluated through 5 items, where high scores reflect higher exposure (Bernstein et al., 2003). NCS were assessed through the Cognition Questionnaire (CQ) (Fennell and Campbell, 1984), which provides a fine-tuned evaluation of negative thinking in response to positive, neutral, and negative events (Fennell and Campbell, 1984). Five different dimensions of NCS can be derived: emotional impact, attribution of causality, generalization across time, generalization across situations, and perceived uncontrollability. High scores in each domain reflect high degree of that specific cognitive distortion.

MRI data acquisition, processing and features extraction

The acquisition of T1-weighted, diffusion tensor imaging (DTI), and resting-state fMRI images was performed with two different 3.0 Tesla scanners. Details about acquisitions parameters for each scanner are reported in **Methods S2**.

The processing of T1-weighted neuroanatomical images was performed through the Computational Anatomy Toolbox (CAT12) for statistical parametric mapping (SPM) software (Gaser et al., 2024). The main pre-processing steps involved: normalization in the Montreal Neurological Institute (MNI) space; tissue

segmentation into GM, WM, and cerebrospinal fluid (CSF); check of spatial alignment and sample homogeneity to exclude outliers; spatial smoothing of each GM map with a 6 mm full width at half maximum Gaussian filter. CT was computed for 68 regions derived from the Desikan-Killiany atlas (Desikan et al., 2006), while cortical and subcortical regional volumes were extracted for 122 regions identified from the Neuromorphometrics atlas (http://Neuromorphometrics.com/). The total intracranial volume (TIV) was also computed.

DTI pre-processing was performed using FMRIB Software Library (FSL) 6.0 tools (Smith et al., 2006, 2004; Woolrich et al., 2009). All images were corrected for eddy currents and head motion (Horsfield, 1999) and skull-stripped (Smith, 2002). Non-linear registration to the FMRIB58-FA template was performed, and a diffusion tensor model was fitted at each voxel to obtain voxel-wise maps of fractional anisotropy (FA), axial (AD), radial (RD), and mean diffusivity (MD). The obtained images were then processed using FSL's Tract Based Spatial Statistics analytic method and aligned to the MNI space through the Non-Linear Image Registration Tool (FNIRT). For each DTI index, the maps of all subjects were merged into a common 4D image, and a "thinning" process was applied to create a skeletonized mean image representing the centers of all common tracts. A threshold of 0.2 was set for this image to control for inter-subject variability and reduce the likelihood of a partial volume effect. Whole-brain tract-based average values for each diffusion index were extracted according to ENIGMA-DTI protocols. Average FA values were calculated from voxels in each subject's white matter skeleton within 43 tract-wise ROIs, derived from the Johns Hopkins University parcellation atlas (Mori et al., 2008). The same procedure was performed for the extraction of tract-based average values of AD, RD and MD. All measures were separately calculated for the right and left hemispheres in each tract, except for midline structures.

The T2*-weighted images were analyzed using the Harmonized AnaLysis of Functional MRI pipeline (HALFpipe) version 1.2.1 (Waller et al., 2022). Pre-processing steps encompass motion correction, slice time correction, susceptibility distortion correction, coregistration, and spatial normalization to the MNI152NLin2009cAsym template. Denoising was performed on the resampled images and included: spatial smoothing with a 6 mm full-width at half-maximum kernel; grand mean scaling of 10,000; ICA-AROMA (Pruim et al., 2015a, 2015b); and temporal filtering using a Gaussian weighted high-pass (width of 125 s) for FC and a frequency-based bandpass (0.01-0.1 Hz) for measures of local neural activity. Physiological nuisance regressors were isolated for anatomical component correction (aCompCor) considering the top 5 CSF principal components (Muschelli et al., 2014). Several resting-state fMRI features were calculated. Considering FC, the time series from 246 Brainnetome (Fan et al., 2016) and 17 cerebellar regions of interest (ROIs) were extracted (Buckner et al., 2011). ROIs with missing time series across participants were excluded, resulting in 186 ROIs (**Table S1**). From the individual ROI-to-ROI FC matrices, positive (Spos) and negative (Sneg) strengths (i.e., the sum of positive and negative weights of links connected to a region) were computed for each ROI using the Python-equivalent of the Brain Connectivity Toolbox (bctpy, https://github.com/aestrivex/bctpy). Local activity metrics included the fractional amplitude of low frequency fluctuations (fALFF) and regional homogeneity (ReHo), calculated from the pre-processed

images. fALFF was defined as the ratio of low frequencies (0.01–0.1 Hz) to the entire frequency power (Zou et al., 2008). ReHo measures the temporal synchronization of a voxel with its nearest neighboring voxels, calculated using the Kendall's coefficient of concordance (Zang et al., 2004). Voxel-wise fALFF and ReHo maps for each participant were Z-standardized, and the corresponding average values across 186 ROIs were extracted.

To account for inter-scanner variability, ComBat harmonization (Johnson et al., 2007) was performed for each neuroimaging feature using neuroCombat (https://github.com/Jfortin1/ComBatHarmonization/tree/master), considering age, sex, diagnosis, and TIV (for GM and CT) as biological covariates to be preserved.

Unsupervised machine learning analysis

To uncover biologically-driven subtypes of depression, a stability-based relative clustering validation algorithm (*NeuReval* Python package) (Colombo et al., 2024; Landi et al., 2021) was implemented for each neuroimaging modality (**Figure 1B**). This method leverages cross-validation to evaluate clustering generalizability by embedding unsupervised clustering in a supervised learning framework (Lange et al., n.d.). For all the models, input features were standardized, and confounding effects (age, sex, pharmacological load, frequency of episodes, and TIV for GM and CT) were regressed out, including age^2 and age-by-sex interaction to account for non-linear effects (Alfaro-Almagro et al., 2021). All these steps were fitted on the training set and then applied to the test set. A 2-fold cross-validation scheme (50% training, 50% test) was employed to account for size imbalances resulting from training-test sets splitting (Landi et al., 2021), and it was repeated 100 times to ensure robustness. For all the models, K-Means was implemented for clustering, while Support Vector Machine (SVM) served as supervised classifier. A grid search procedure was performed for hyperparameters tuning, using the minimization of the normalized stability as the criterion to select the optimal ones. These included K-Means initialization (random or k-means++), the soft-margin C (range: 0.01, 0.1, 1, 10, 100, 1000), and kernel type (linear or radial basis function) for SVM. Clustering solutions were evaluated for 2 to 5 clusters, and the one achieving the minimum normalized stability throughout cross-validation was selected.

To investigate whether the combination of different neuroimaging modalities improved stratification over single-modality models, a multiview spectral clustering algorithm was embedded within the *NeuReval* pipeline (https://github.com/fede-colombo/Multiview_NeuReval). In multiview frameworks, different feature sets ("views") are entered within the clustering algorithm, which can be separately used to derive clusters. The rationale behind this approach is that the grouping structure identified in one view should agree with the one derived from another view. The best clustering solution is the one that assigns an observation to the same cluster regardless of the specific view (Kumar and Daumé, 2011). Only modalities that resulted in stable solutions in single-modality models were included, considering the same cross-validation scheme and confounds controls. Tuned hyperparameters included the affinity matrix (radial basis function or nearest neighbors) for multiview spectral clustering and SVM hyperparameters.

The internal quality of clustering solutions was further assessed with the Silhouette score and the Davies-Bouldin index. Statistical significance was tested with 10,000 Monte Carlo simulations using the *sigclust* method (R library) (Liu et al., 2008). Only stratification models that passed false-discovery rate (FDR) q<0.05 threshold were deemed as significant.

Univariate and multivariate characterization of the clusters

For each significant model, clusters were compared for age, diagnosis, sex, number of previous episodes, years of education, age of onset, duration of illness, pharmacological load, HDRS-21 total score, CTQ and CQ total scores and domains. The same approach was employed for neuroimaging features. Cohen's d effects sizes were calculated and multiple comparisons were FDR-corrected (q<0.05). Comparisons with HC were conducted only for the best-performing model. Cluster assignment agreement across models was assessed with the Fleiss' kappa statistic.

For each significant stratification model, grouped partial least squares correlation (PLSC) analyses were also performed to investigate whether the multivariate neurobiological-ACEs relationship was different between clusters (myPLS MATLAB toolbox, https://github.com/danizoeller/myPLS/). (**Figure 1 D-E**). PLSC is a multivariate technique that identifies latent variable (LV) pairs capturing shared variance between two datasets (e.g., brain and behavioral data). With group labels, PLSC computes separate covariance matrices, enabling detection of between-cluster differences in multivariate brain–behavior associations (Krishnan et al., 2011). Prior to analyses, neuroimaging variables were residualized for the same confounds considered for *NeuReval*. CTQ scores were adjusted for age, sex, and education. For each model, 5000 permutations were performed to assess the statistical significance of the LV pairs (FDR q<0.05). Brain bootstrap ratio (BSR) and 95% confidence intervals (CI) on neurobiological-ACEs correlations were estimated through 5000 bootstrap resampling. BSRs were computed by dividing the correlation coefficient for each biological variable by its bootstrapped standard deviation, and interpreted as standardized weights (Krishnan et al., 2011). BSRs>|2| were judged as important in guiding the neurobiological-ACEs relationships, whereas CTQ loadings with 95% CI that do not include zero were deemed as significant. BSRs were converted into p-values and FDR-corrected (q<0.05) (Kebets et al., 2019).

For significant LV pairs, multivariate general linear models (GLMs) were implemented separately for each cluster, with LV neurobiological scores predicting CQ domains. Univariate analyses were also performed within each cluster to explore the effect of LV neurobiological scores on each CQ domain. Statistical significance was assessed using parametric estimates of the predictor variables, calculated by the least squares method. For those CQ domains that were significantly predicted by LV neurobiological scores, mediation models were performed, considering LV CTQ scores as independent variables, LV neurobiological scores as mediator, and CQ domain as dependent variable (5000 bootstraps, 90% CI) (SPSS PROCESS macro) (Hayes, 2012). (**Figure 1F**).

Results

Descriptive statistics of the whole sample (N=482) are reported in **Table 1**. No significant differences in age, sex, duration of illness, and pharmacological load were observed between MDD and BD. However, BD patients showed a significantly higher number of previous episodes compared to MDD ($q<0.001$). BD and MDD patients were also comparable for HDRS-21, CQ and CTQ domains. HC were younger, with higher level of education and lower CTQ and CQ scores compared to both MDD and BD. In the whole sample, significant and positive correlations were found across all the CTQ and CQ domains (**Figure S1**).

Performances of stratification models

Models based on structural neuroimaging, FC or multimodal data showed good accuracies in clusters' differentiation, identifying two clusters of patients as the optimal clustering solution (accuracy range: 73.4%-84.8%, $q<0.05$). Models trained exclusively on ReHo and fALFF modality did not achieve a predictive accuracy above chance level or significance (**Table 2** and **Figure S2**). The best clustering performance was observed for the FC-based model, showing an accuracy in discriminating clusters of 84.8%. Fleiss' kappa statistic was $k=0.07$, suggesting a low agreement across stratification models in assigning subjects to the same cluster.

Neurobiological characterization of data-driven clusters

All the stratification models distinguished between a cluster of depressed patients with a more preserved brain structure or function and a second one characterized by a more compromised brain signature. Considering the FC-based clusters, Cluster 1 exhibited higher Spos compared to Cluster 2, with the largest effect sizes found in the cingulate gyrus, precuneus, and superior frontal gyrus (SFG). Conversely, Cluster 2 showed overall higher Sneg compared to Cluster 1, despite reduced effect sizes compared to Cluster 1 (**Figure 2**). Similarly, GM and CT-based models uncovered a cluster of depressed patients marked by widespread volumetric reductions and cortical thinning, with the main effects localized in temporo-parietal regions (**Figure S3**). All the DTI-based models uncovered one cluster differing from the second one in opposite direction, with the largest contributions in the corpus callosum and corona radiata (**Figure S4**). When combing all modalities in the multimodal stratification model, clusters' differentiation was mainly guided by DTI measures, with one cluster exhibited higher RD, MD, AD, and lower FA values compared to the other (**Figure S5**).

To clarify the direction of neurobiological alterations in the best-performing stratification model (i.e., FC-based), we examined differences in global and regional Spos and Sneg measures between clusters and HC. At the global level, patients in Cluster 1 showed significantly higher Spos compared to both Cluster 2 and HC, while patients belonging to Cluster 2 exhibited elevated Sneg relative to Cluster 1 and HC (**Figure 3A-B**). Evidence of group differences in Spos or Sneg was also observed across individual brain regions, consistent with the patterns described at the global level (**Table S13**). These results generally indicate that Cluster 1 is distinguished by an increased functional integration, while an abnormal functional segregation

characterize Cluster 2.

Differential neurobiological-ACEs associations between clusters

A significant LV pair surviving FDR correction was obtained only for the FC-based model (explained covariance=40.0%, q=0.01) (**Table S11**). The largest BSR were observed for ROIs in the ventral and caudal part of the cingulate gyrus, superior and inferior parietal lobules, insula, somatosensory cortex, as well as the lateral amygdala, thalamus, and basal ganglia, and these effects were found for both Spos and Sneg (**Figure 4A-B**). In Cluster 1 all CTQ domains, except for sexual abuse, significantly contributed to the neurobiological-ACEs multivariate association. The direction of CTQ loadings was negative, meaning that higher exposure to childhood trauma is associated with decreased FC strength. In Cluster 2, negative significant associations emerged for emotional neglect, while positive for sexual abuse. (**Figure 4C**). PLS analysis including HC produced similar results, isolating a significant LV pair (explained covariance=43.0%, q=0.015) (**Table S12**). The contribution of CTQ domains to the neurobiological–ACEs association was highly similar between HC and Cluster 1, whereas only the domains of sexual and physical abuse were significant in Cluster 2. Thus, the identified LV likely reflects a normative neurobiological–ACEs relationship that is present in HC and preserved in Cluster 1, but absent in Cluster 2 (**Figure S6**).

When considering univariate analyses, patients belonging to the FC-based Cluster 2 showed higher scores in generalization across events and perceived uncontrollability, while a trend toward significance was found for sexual abuse. However, these results did not survive FDR correction (**Table S2**). Compared to HC, both clusters exhibited higher scores in attribution of causality, generalization across events, and CQ total score. However, only Cluster 2 showed higher scores in sexual abuse, CTQ total score, generalization across time, and perceived uncontrollability relative to HC (**Table S10**). At an uncorrected p-values, significant differences in diagnosis were found for clusters derived from AD, while a trend toward significance was detected in the FA-based clusters. No significant differences were detected for clusters derived from GM and CT (**Tables S3-S9**).

Effect of FC strength on cognitive distortions in the FC-based clusters

The final step was to explore whether the LV FC scores differentially mediated the relationships between the LV CTQ scores and CQ domains in the FC-based clusters. Multivariate GLMs did not show significant effects for LV FC scores on CQ domains neither in Cluster 1 (Wilk's λ=0.88, F(5,27)=0.73, p=0.612) nor in Cluster 2 (Wilk's λ=0.87, F(5,58)=1.71, p=0.147). Considering univariate results, LV FC scores significantly and positively predicted generalization across time only in Cluster 2 (b=0.029, p=0.032; overall model fit: R2=0.07, RMSE=0.90, F(1,62)=4.85, p=0.031). Mediation analysis revealed a significant indirect effect of LV CTQ scores on generalization across time through LV FC scores (i.e., path a*b). The total and the direct effects of LV CTQ scores on generalization across time were not significant; however, the significant indirect effect support the mediation effect of LV FC scores. LV CTQ scores significantly increased LV FC scores (path a), whereas the effect of LV FC scores on generalization across time is marginally significant (path b). These results suggest that in Cluster 2 LV FC scores significantly mediate the relationship between

LV CTQ scores and generalization across time, despite the total effect is not significant (**Figure 4D)**.

Discussion

This study explored whether multimodal neuroimaging could support clinically meaningful data-driven stratifications of depressive mood disorders. Among all tested models, the highest accuracy was observed for the FC-based model (85%), uncovering two transdiagnostic biotypes: one characterized by widespread high positive FC strength (Cluster 1, N=50), while another one by dominant negative FC strength (Cluster 2, N=96). Importantly, differential neurobiological-ACEs associations in the FC-based clusters emerged. In Cluster 1, childhood trauma was negatively associated with FC in the cingulate gyrus, insula, somatosensory cortex, and subcortical regions, consistent with the ACEs-related pattern also observed in HC. In Cluster 2, emotional neglect was linked to reduced FC, while sexual abuse showed a positive association. ACEs-related FC mediated the relationship between ACEs and NCS of overgeneralization in this latter cluster, supporting biotype-specific neurobiological pathways linking early trauma and cognitive vulnerability.

The functional profiles of the discovered biotypes reflect widespread connectome alterations characterized by differential contribution of positive and negative FC strength. While positive correlations may reflect synchronized neural activity, the biological meaning of negative correlations is still debated (Goelman et al., 2014; Zhan et al., 2017). However, the strength of negative correlations among brain regions has been shown to be directly correlated with the length of their shortest path, thus reflecting less efficient information flow (Chen et al., 2011). The lack of balance between functional integration and segregation is well-documented in psychiatric disorders, possibly reflecting a shift toward a more random and less integrated network configuration (de Lange et al., 2019; Hansen et al., 2022; Repple et al., 2023; Xia et al., 2019). Our findings extend this scenario by demonstrating that this unbalance manifests as distinct biotypes within depression, differing from HC in global and regional FC.

A significant neurobiological-ACEs relationship was differentially present in the two FC biotypes. The regions most affected by ACEs (amygdala, cingulate, thalamus, basal ganglia, insula, sensorimotor areas), are crucial for emotional, cognitive and social functioning, and their functional organization is highly influenced by cortical maturational changes (Casey et al., 2019; Dong et al., 2024; Luo et al., 2024; Park et al., 2024). The deprivation of adequate emotional stimulation during childhood disrupts these processes by diminishing neurotrophin and neurotransmitters production which, ultimately, end with aberrant neural organization (De Bellis, 2005; van der Kolk, 2003). Among all the CTQ domains, sexual abuse emerged as a key discriminating factor between the two biotypes and HC, showing a significant and positive association with FC only in Cluster 2. Given the negative FC strength characterizing this biotype, exposure to childhood abuse would be expected to further reduce FC. However, this association may reflect a compensatory mechanism, consistent with the stress acceleration hypothesis, whereby early adversities accelerate the maturation of brain circuits involved in salience detection and executive functions to promote short-term adaptations (Callaghan and Tottenham, 2016; Holz et al., 2023). These findings may point to a more severely affected subgroup, where localized increases in functional coupling compensate for abuse-related widespread connectivity deficits.

The presence of distinct underlying mechanisms is further supported by the mediation analysis, where the

ACE-related FC scores mediated the relationship between the ACEs and generalization across time only in the hyper-segregated biotype. Overgeneralization represents a key feature of depressive symptomatology (Gamble et al., 2019), and constitutes a core element of the depressive "cognitive triad" (Beck, 2008). While ACEs are established risk factors for NCS (Alaftar and Uzer, 2022; Mansueto et al., 2021; Poletti et al., 2014a), these results suggest that the tendency to overgeneralize might characterize a specific neurobiological subtype of depressed patients, which may benefit from cognitive or trauma-focused psychotherapies (Cohen and Mannarino, 2015; Wiles et al., 2013).

Unlike the FC-based biotypes, structural MRI models did not reveal significant associations with ACEs or NCS, though they reliably distinguished patients with widespread WM dysconnectivity, cortical thinning and volumetric reductions (accuracies > 70%). These alterations may reflect diagnosis-specific effects, consistent with evidence that GM and DTI metrics differentiate BD and MDD with accuracies up to 78% (Calesella et al., 2024; Colombo et al., 2022; Vai et al., 2020). Accordingly, clusters derived from FA and AD exhibited trends toward a significant difference for diagnosis, although not surviving FDR correction. Conversely, this association was not found for the FC-based clusters, suggesting that functional measures are more likely to reflect transdiagnostic signatures rather that clinical diagnoses (Goldstein-Piekarski et al., 2022; Tozzi et al., 2024; Williams, 2017). Alternatively, the limited overlap with FC clusters may reflect distinct pathological dimensions captured solely by structural modalities, such as immune-inflammatory mechanisms or cognitive deficits (Colombo et al., 2024; Liang et al., 2019). The low overlapping between structural and functional clustering solutions might also explain why the multimodal stratification model did not outperform the FC-based one, despite achieving a moderate classification performance (73.4%) and the best internal validity (Silhouette and Davies-Bouldin scores).

Some limitations should be underscored. All patients were inpatients admitted to the same hospital, limiting generalizability. Although pharmacological load was statistically controlled, residual long-lasting effects cannot be completely ruled out. Finally, the modest sample size and lack of additional biological measures (e.g., genetic or inflammatory markers) may have constrained detection of more nuanced associations.

In conclusion, this work shows that FC-based biotypes best captured distinct trauma-related neurobiological profiles in depression. One biotype exhibited hyperconnectivity and negative associations with ACEs; the other, characterized by network segregation, showed a more specific pattern involving sexual abuse, emotional neglect, and overgeneralization. These findings highlight the potential of FC to define transdiagnostic depression subtypes with differential vulnerability to early adversity, informing a neurobiologically grounded taxonomy of mood disorders.

Acknowledgments

None.

Funding sources

This study was supported by the Italian Ministry of Health (grant numbers GR 2019-12370616).

References

Alaftar, İ., Uzer, T., 2022. Understanding intergenerational transmission of early maladaptive schemas from a memory perspective: Moderating role of overgeneral memory on adverse experiences. Child Abuse Negl. 127, 105539. https://doi.org/10.1016/j.chiabu.2022.105539

Alfaro-Almagro, F., McCarthy, P., Afyouni, S., Andersson, J.L.R., Bastiani, M., Miller, K.L., Nichols, T.E., Smith, S.M., 2021. Confound modelling in UK Biobank brain imaging. Neuroimage 224, 117002. https://doi.org/10.1016/j.neuroimage.2020.117002

Beck, A.T., 2008. Reviews and Overviews The Evolution of the Cognitive Model of Depression and Its Neurobiological Correlates, Am J Psychiatry.

Benedetti, F., Bollettini, I., Radaelli, D., Poletti, S., Locatelli, C., Falini, A., Smeraldi, E., Colombo, C., 2014. Adverse childhood experiences influence white matter microstructure in patients with bipolar disorder. Psychol. Med. 44, 3069–3082. https://doi.org/10.1017/S0033291714000506

Benedetti, F., Poletti, S., Radaelli, D., Pozzi, E., Giacosa, C., Ruffini, C., Falini, A., Smeraldi, E., 2012. Caudate gray matter volume in obsessive-compulsive disorder is influenced by adverse childhood experiences and ongoing drug treatment. J. Clin. Psychopharmacol. 32, 544–547. https://doi.org/10.1097/JCP.0b013e31825cce05

Benedetti, F., Radaelli, D., Poletti, S., Falini, A., Cavallaro, R., Dallaspezia, S., Riccaboni, R., Scotti, G., Smeraldi, E., 2011. Emotional reactivity in chronic schizophrenia: structural and functional brain correlates and the influence of adverse childhood experiences. Psychol. Med. 41, 509–519. https://doi.org/10.1017/S0033291710001108

Bernstein, D.P., Stein, J.A., Newcomb, M.D., Walker, E., Pogge, D., Ahluvalia, T., Stokes, J., Handelsman, L., Medrano, M., Desmond, D., 2003. Development and validation of a brief screening version of the Childhood Trauma Questionnaire. Child Abuse Negl. 27, 169–190.

Blair, D.-L., Kingsbury, M., Eccles, H., Akther, A., Siddiqi, S., Condran, G., Obeegadoo, I., Murray, J., Geoffroy, M.-C., Menezes, A.M.B., Sikora, L., Colman, I., 2025. Adverse childhood experiences and suicidality in low-income and middle-income countries: a systematic review and meta-analysis. BMJ Glob. Health 10, e018129. https://doi.org/10.1136/bmjgh-2024-018129

Buckner, R.L., Krienen, F.M., Castellanos, A., Diaz, J.C., Yeo, B.T., 2011. The organization of the human cerebellum estimated by intrinsic functional connectivity. J. Neurophysiol. 106, 2322–2345.

Bzdok, D., Meyer-Lindenberg, A., 2018. Machine Learning for Precision Psychiatry: Opportunities and Challenges. Biol. Psychiatry Cogn. Neurosci. Neuroimaging. https://doi.org/10.1016/j.bpsc.2017.11.007

Calesella, F., Colombo, F., Bravi, B., Fortaner-Uyà, L., Monopoli, C., Poletti, S., Tassi, E., Maggioni, E., Brambilla, P., Colombo, C., Bollettini, I., Benedetti, F., Vai, B., 2024. A machine learning pipeline for efficient differentiation between bipolar and major depressive disorder based on multimodal structural neuroimaging. Neurosci. Appl. 3, 103931. https://doi.org/10.1016/j.nsa.2023.103931

Callaghan, B.L., Tottenham, N., 2016. The Stress Acceleration Hypothesis: Effects of early-life adversity on emotion circuits and behavior. Curr. Opin. Behav. Sci. 7, 76–81. https://doi.org/10.1016/j.cobeha.2015.11.018

Casey, B.J., Heller, A.S., Gee, D.G., Cohen, A.O., 2019. Development of the emotional brain. Neurosci. Lett. 693, 29–34. https://doi.org/10.1016/j.neulet.2017.11.055

Chen, Guangyu, Chen, Gang, Xie, C., Li, S.-J., 2011. Negative functional connectivity and its dependence on the shortest path length of positive network in the resting-state human brain. Brain Connect. 1, 195–206. https://doi.org/10.1089/brain.2011.0025

Cirone, C., Secci, I., Favole, I., Ricci, F., Amianto, F., Davico, C., Vitiello, B., 2021. What Do We Know about the Long-Term Course of Early Onset Bipolar Disorder? A Review of the Current Evidence. Brain Sci. 11. https://doi.org/10.3390/brainsci11030341

Cohen, J.A., Mannarino, A.P., 2015. Trauma-focused Cognitive Behavior Therapy for Traumatized Children and Families. Child Adolesc. Psychiatr. Clin. N. Am. 24, 557–70. https://doi.org/10.1016/j.chc.2015.02.005

Colombo, F., Calesella, F., Bravi, B., Fortaner-Uyà, L., Monopoli, C., Tassi, E., Carminati, M., Zanardi, R., Bollettini, I., Poletti, S., Lorenzi, C., Spadini, S., Brambilla, P., Serretti, A., Maggioni, E., Fabbri, C., Benedetti, F., Vai, B., 2024. Multimodal brain-derived subtypes of Major depressive disorder differentiate patients for anergic symptoms, immune-inflammatory markers, history of childhood

trauma and treatment-resistance. Eur. Neuropsychopharmacol. 85, 45–57. https://doi.org/10.1016/j.euroneuro.2024.05.015

Colombo, F., Calesella, F., Mazza, M.G., Melloni, E.M.T., Morelli, M.J., Scotti, G.M., Benedetti, F., Bollettini, I., Vai, B., 2022. Machine learning approaches for prediction of bipolar disorder based on biological, clinical and neuropsychological markers: A systematic review and meta-analysis. Neurosci. Biobehav. Rev. 135. https://doi.org/10.1016/j.neubiorev.2022.104552

De Bellis, M.D., 2005. The psychobiology of neglect. Child Maltreat. 10, 150–172.

de Lange, S.C., Scholtens, L.H., van den Berg, L.H., Boks, M.P., Bozzali, M., Cahn, W., Dannlowski, U., Durston, S., Geuze, E., van Haren, N.E.M., Hillegers, M.H.J., Koch, K., Jurado, M.Á., Mancini, M., Marqués-Iturria, I., Meinert, S., Ophoff, R.A., Reess, T.J., Repple, J., Kahn, R.S., van den Heuvel, M.P., 2019. Shared vulnerability for connectome alterations across psychiatric and neurological brain disorders. Nat. Hum. Behav. 3, 988–998. https://doi.org/10.1038/s41562-019-0659-6

Desikan, R.S., Ségonne, F., Fischl, B., Quinn, B.T., Dickerson, B.C., Blacker, D., Buckner, R.L., Dale, A.M., Maguire, R.P., Hyman, B.T., Albert, M.S., Killiany, R.J., 2006. An automated labeling system for subdividing the human cerebral cortex on MRI scans into gyral based regions of interest. NeuroImage 31, 968–980. https://doi.org/10.1016/j.neuroimage.2006.01.021

Dong, H.-M., Zhang, X.-H., Labache, L., Zhang, S., Ooi, L.Q.R., Yeo, B.T.T., Margulies, D.S., Holmes, A.J., Zuo, X.-N., 2024. Ventral attention network connectivity is linked to cortical maturation and cognitive ability in childhood. Nat. Neurosci. https://doi.org/10.1038/s41593-024-01736-x

Drysdale, A.T., Grosenick, L., Downar, J., Dunlop, K., Mansouri, F., Meng, Y., Fetcho, R.N., Zebley, B., Oathes, D.J., Etkin, A., Schatzberg, A.F., Sudheimer, K., Keller, J., Mayberg, H.S., Gunning, F.M., Alexopoulos, G.S., Fox, M.D., Pascual-Leone, A., Voss, H.U., Casey, B.J., Dubin, M.J., Liston, C., 2017. Resting-state connectivity biomarkers define neurophysiological subtypes of depression. Nat. Med. 23, 28–38. https://doi.org/10.1038/nm.4246

Fan, L., Li, H., Zhuo, J., Zhang, Y., Wang, J., Chen, L., Yang, Z., Chu, C., Xie, S., Laird, A.R., 2016. The human brainnetome atlas: a new brain atlas based on connectional architecture. Cereb. Cortex 26, 3508–3526.

Fazakas-DeHoog, L.L., Rnic, K., Dozois, D.J.A., 2017. A Cognitive Distortions and Deficits Model of Suicide Ideation. Eur. J. Psychol. 13, 178–193. https://doi.org/10.5964/ejop.v13i2.1238

Fennell, M.J.V., Campbell, E.A., 1984. The cognitions questionnaire: Specific thinking errors in depression. Br. J. Clin. Psychol. 23, 81–92. https://doi.org/10.1111/j.2044-8260.1984.tb00631.x

Fernandes, B.S., Williams, L.M., Steiner, J., Leboyer, M., Carvalho, A.F., Berk, M., 2017. The new field of "precision psychiatry." BMC Med. 15. https://doi.org/10.1186/s12916-017-0849-x

Gamble, B., Moreau, D., Tippett, L.J., Addis, D.R., 2019. Specificity of Future Thinking in Depression: A Meta-Analysis. Perspect. Psychol. Sci. 14, 816–834. https://doi.org/10.1177/1745691619851784

Gaser, C., Dahnke, R., Thompson, P.M., Kurth, F., Luders, E., the Alzheimer's Disease Neuroimaging Initiative, 2024. CAT: a computational anatomy toolbox for the analysis of structural MRI data. GigaScience 13, giae049. https://doi.org/10.1093/gigascience/giae049

GBD Mental Disorders Collaborators, 2022. Global, regional, and national burden of 12 mental disorders in 204 countries and territories, 1990-2019: a systematic analysis for the Global Burden of Disease Study 2019. Lancet Psychiatry 9, 137–150. https://doi.org/10.1016/S2215-0366(21)00395-3

Giampetruzzi, E., Tan, A.C., LoPilato, A., Kitay, B., Riva Posse, P., McDonald, W.M., Hermida, A.P., Crowell, A., Hershenberg, R., 2023. The impact of adverse childhood experiences on adult depression severity and treatment outcomes. J. Affect. Disord. 333, 233–239. https://doi.org/10.1016/j.jad.2023.04.071

Goldstein-Piekarski, A.N., Ball, T.M., Samara, Z., Staveland, B.R., Keller, A.S., Fleming, S.L., Grisanzio, K.A., Holt-Gosselin, B., Stetz, P., Ma, J., Williams, L.M., 2022. Mapping Neural Circuit Biotypes to Symptoms and Behavioral Dimensions of Depression and Anxiety. Biol. Psychiatry 91, 561–571. https://doi.org/10.1016/j.biopsych.2021.06.024

Hamilton, M., 1986. The Hamilton rating scale for depression, in: Assessment of Depression. Springer, pp. 143–152.

Hansen, J.Y., Shafiei, G., Vogel, J.W., Smart, K., Bearden, C.E., Hoogman, M., Franke, B., van Rooij, D., Buitelaar, J., McDonald, C.R., Sisodiya, S.M., Schmaal, L., Veltman, D.J., van den Heuvel, O.A., Stein, D.J., van Erp, T.G.M., Ching, C.R.K., Andreassen, O.A., Hajek, T., Opel, N., Modinos, G.,

Aleman, A., van der Werf, Y., Jahanshad, N., Thomopoulos, S.I., Thompson, P.M., Carson, R.E., Dagher, A., Misic, B., 2022. Local molecular and global connectomic contributions to cross-disorder cortical abnormalities. Nat. Commun. 13, 4682. https://doi.org/10.1038/s41467-022-32420-y

Hayashi, Y., Okamoto, Y., Takagaki, K., Okada, G., Toki, S., Inoue, T., Tanabe, H., Kobayakawa, M., Yamawaki, S., 2015. Direct and indirect influences of childhood abuse on depression symptoms in patients with major depressive disorder. BMC Psychiatry 15, 244. https://doi.org/10.1186/s12888-015-0636-1

Hayes, A.F., 2012. PROCESS□: A Versatile Computational Tool for Observed Variable Mediation , Moderation , and Conditional Process Modeling 1.

Holz, N.E., Berhe, O., Sacu, S., Schwarz, E., Tesarz, J., Heim, C.M., Tost, H., 2023. Early Social Adversity, Altered Brain Functional Connectivity, and Mental Health. Biol. Psychiatry, Making Connections: Biological Mechanisms of Human Brain (Dys)connectivity 93, 430–441. https://doi.org/10.1016/j.biopsych.2022.10.019

Horsfield, M.A., 1999. Mapping eddy current induced fields for the correction of diffusion-weighted echo planar images. Magn. Reson. Imaging 17, 1335–1345. https://doi.org/10.1016/S0730-725X(99)00077-6

Johnson, W.E., Li, C., Rabinovic, A., 2007. Adjusting batch effects in microarray expression data using empirical Bayes methods. Biostatistics 8, 118–127. https://doi.org/10.1093/biostatistics/kxj037

Jones, E.B., Sharpe, L., 2017. Cognitive bias modification: A review of meta-analyses. J. Affect. Disord. 223, 175–183. https://doi.org/10.1016/j.jad.2017.07.034

Kebets, V., Holmes, A.J., Orban, C., Tang, S., Li, J., Sun, N., Kong, R., Poldrack, R.A., Yeo, B.T.T., 2019. Somatosensory-Motor Dysconnectivity Spans Multiple Transdiagnostic Dimensions of Psychopathology. Biol. Psychiatry 86, 779–791. https://doi.org/10.1016/j.biopsych.2019.06.013

Kendall, K.M., Van Assche, E., Andlauer, T.F.M., Choi, K.W., Luykx, J.J., Schulte, E.C., Lu, Y., 2021. The genetic basis of major depression. Psychol. Med. 51, 2217–2230. https://doi.org/10.1017/S0033291721000441

Krishnan, A., Williams, L.J., McIntosh, A.R., Abdi, H., 2011. Partial Least Squares (PLS) methods for neuroimaging: A tutorial and review. NeuroImage 56, 455–475. https://doi.org/10.1016/j.neuroimage.2010.07.034

Kumar, A., Daumé, H., 2011. A co-training approach for multi-view spectral clustering. Presented at the Proceedings of the 28th international conference on machine learning (ICML-11), pp. 393–400.

Landi, I., Mandelli, V., Lombardo, M.V., 2021. reval: A Python package to determine best clustering solutions with stability-based relative clustering validation. Patterns 2. https://doi.org/10.1016/j.patter.2021.100228

Lange, T., Roth, V., Braun, M.L., Buhmann, J.M., n.d. Stability-Based Validation of Clustering Solutions.

Liang, S., Deng, W., Li, X., Greenshaw, A.J., Wang, Q., Li, M., Ma, X., Bai, T.J., Bo, Q.J., Cao, J., Chen, G.M., Chen, W., Cheng, C., Cheng, Y.Q., Cui, X.L., Duan, J., Fang, Y.R., Gong, Q.Y., Guo, W.B., Hou, Z.H., Hu, L., Kuang, L., Li, F., Li, K.M., Liu, Y.S., Liu, Z.N., Long, Y.C., Luo, Q.H., Meng, H.Q., Peng, D.H., Qiu, H.T., Qiu, J., Shen, Y.D., Shi, Y.S., Si, T.M., Wang, C.Y., Wang, F., Wang, K., Wang, L., Wang, X., Wang, Y., Wu, X.P., Wu, X.R., Xie, C.M., Xie, G.R., Xie, H.Y., Xie, P., Xu, X.F., Yang, H., Yang, J., Yu, H., Yao, J.S., Yao, S.Q., Yin, Y.Y., Yuan, Y.G., Zang, Y.F., Zhang, A.X., Zhang, H., Zhang, K.R., Zhang, Z.J., Zhao, J.P., Zhou, R.B., Zhou, Y.T., Zou, C.J., Zuo, X.N., Yan, C.G., Li, T., 2020. Biotypes of major depressive disorder: Neuroimaging evidence from resting-state default mode network patterns. NeuroImage Clin. 28. https://doi.org/10.1016/j.nicl.2020.102514

Liang, S., Wang, Q., Kong, X., Deng, W., Yang, X., Li, Xiaojing, Zhang, Z., Zhang, J., Zhang, C., Li, Xin min, Ma, X., Shao, J., Greenshaw, A.J., Li, T., 2019. White Matter Abnormalities in Major Depression Biotypes Identified by Diffusion Tensor Imaging. Neurosci. Bull. 35, 867–876. https://doi.org/10.1007/s12264-019-00381-w

Liu, Y., Hayes, D.N., Nobel, A., Marron, J.S., 2008. Statistical significance of clustering for high-dimension, low-sample size data. J. Am. Stat. Assoc. 103, 1281–1293. https://doi.org/10.1198/016214508000000454

Luo, A.C., Sydnor, V.J., Pines, A., Larsen, B., Alexander-Bloch, A.F., Cieslak, M., Covitz, S., Chen, A.A., Esper, N.B., Feczko, E., Franco, A.R., Gur, R.E., Gur, R.C., Houghton, A., Hu, F., Keller, A.S., Kiar, G., Mehta, K., Salum, G.A., Tapera, T., Xu, T., Zhao, C., Salo, T., Fair, D.A., Shinohara, R.T.,

Milham, M.P., Satterthwaite, T.D., 2024. Functional connectivity development along the sensorimotor-association axis enhances the cortical hierarchy. Nat Commun 15, 3511. https://doi.org/10.1038/s41467-024-47748-w

Mansueto, G., Cavallo, C., Palmieri, S., Ruggiero, G.M., Sassaroli, S., Caselli, G., 2021. Adverse childhood experiences and repetitive negative thinking in adulthood: A systematic review. Clin. Psychol. Psychother. https://doi.org/10.1002/cpp.2590

Maslej, M.M., Furukawa, T.A., Cipriani, A., Andrews, P.W., Sanches, M., Tomlinson, A., Volkmann, C., McCutcheon, R.A., Howes, O., Guo, X., Mulsant, B.H., 2021. Individual Differences in Response to Antidepressants: A Meta-analysis of Placebo-Controlled Randomized Clinical Trials. JAMA Psychiatry 78, 490–497. https://doi.org/10.1001/jamapsychiatry.2020.4564

Mori, S., Oishi, K., Jiang, H., Jiang, L., Li, X., Akhter, K., Hua, K., Faria, A.V., Mahmood, A., Woods, R., Toga, A.W., Pike, G.B., Neto, P.R., Evans, A., Zhang, J., Huang, H., Miller, M.I., Van Zijl, P., Mazziotta, J., 2008. Stereotaxic white matter atlas based on diffusion tensor imaging in an ICBM template. NeuroImage 40, 570–582. https://doi.org/10.1016/j.neuroimage.2007.12.035

Muschelli, J., Nebel, M.B., Caffo, B.S., Barber, A.D., Pekar, J.J., Mostofsky, S.H., 2014. Reduction of motion-related artifacts in resting state fMRI using aCompCor. Neuroimage 96, 22–35.

Park, S., Haak, K.V., Oldham, S., Cho, H., Byeon, K., Park, B., Thomson, P., Chen, H., Gao, W., Xu, T., Valk, S., Milham, M.P., Bernhardt, B., Di Martino, A., Hong, S.-J., 2024. A shifting role of thalamocortical connectivity in the emergence of cortical functional organization. Nat. Neurosci. 27, 1609–1619. https://doi.org/10.1038/s41593-024-01679-3

Poletti, S., Aggio, V., Brioschi, S., Bollettini, I., Falini, A., Colombo, C., Benedetti, F., 2018. Impact of early and recent stress on white matter microstructure in major depressive disorder. J. Affect. Disord. 225, 289–297. https://doi.org/10.1016/j.jad.2017.08.017

Poletti, S., Colombo, C., Benedetti, F., 2014a. Adverse childhood experiences worsen cognitive distortion during adult bipolar depression. Compr. Psychiatry 55, 1803–1808. https://doi.org/10.1016/j.comppsych.2014.07.013

Poletti, S., Locatelli, C., Radaelli, D., Lorenzi, C., Smeraldi, E., Colombo, C., Benedetti, F., 2014b. Effect of early stress on hippocampal gray matter is influenced by a functional polymorphism in EAAT2 in bipolar disorder. Prog. Neuropsychopharmacol. Biol. Psychiatry 51, 146–152. https://doi.org/10.1016/j.pnpbp.2014.01.021

Poletti, S., Vai, B., Smeraldi, E., Cavallaro, R., Colombo, C., Benedetti, F., 2016. Adverse childhood experiences influence the detrimental effect of bipolar disorder and schizophrenia on cortico-limbic grey matter volumes. J. Affect. Disord. 189, 290–297. https://doi.org/10.1016/j.jad.2015.09.049

Price, R.B., Gates, K., Kraynak, T.E., Thase, M.E., Siegle, G.J., 2017. Data-Driven Subgroups in Depression Derived from Directed Functional Connectivity Paths at Rest. Neuropsychopharmacology 42, 2623–2632. https://doi.org/10.1038/npp.2017.97

Pruim, R.H., Mennes, M., Buitelaar, J.K., Beckmann, C.F., 2015a. Evaluation of ICA-AROMA and alternative strategies for motion artifact removal in resting state fMRI. Neuroimage 112, 278–287.

Pruim, R.H., Mennes, M., van Rooij, D., Llera, A., Buitelaar, J.K., Beckmann, C.F., 2015b. ICA-AROMA: A robust ICA-based strategy for removing motion artifacts from fMRI data. Neuroimage 112, 267–277.

Repple, J., Gruber, M., Mauritz, M., de Lange, S.C., Winter, N.R., Opel, N., Goltermann, J., Meinert, S., Grotegerd, D., Leehr, E.J., Enneking, V., Borgers, T., Klug, M., Lemke, H., Waltemate, L., Thiel, K., Winter, A., Breuer, F., Grumbach, P., Hofmann, H., Stein, F., Brosch, K., Ringwald, K.G., Pfarr, J., Thomas-Odenthal, F., Meller, T., Jansen, A., Nenadic, I., Redlich, R., Bauer, J., Kircher, T., Hahn, T., van den Heuvel, M., Dannlowski, U., 2023. Shared and Specific Patterns of Structural Brain Connectivity Across Affective and Psychotic Disorders. Biol. Psychiatry, Schizophrenia: Novel Molecular and Circuit Mechanisms 93, 178–186. https://doi.org/10.1016/j.biopsych.2022.05.031

Sackeim, H.A., 2001. The definition and meaning of treatment-resistant depression. J. Clin. Psychiatry 62, 10–17.

Scheepens, D.S., van Waarde, J.A., Ten Doesschate, F., Westra, M., Kroes, M.C.W., Schene, A.H., Schoevers, R.A., Denys, D., Ruhé, H.G., van Wingen, G.A., 2022. Negative cognitive schema modification as mediator of symptom improvement after electroconvulsive therapy in major depressive disorder. J. Affect. Disord. 310, 156–161. https://doi.org/10.1016/j.jad.2022.04.088

Sha, Z., Wager, T.D., Mechelli, A., He, Y., 2019. Common Dysfunction of Large-Scale Neurocognitive Networks Across Psychiatric Disorders. Biol. Psychiatry 85, 379–388. https://doi.org/10.1016/j.biopsych.2018.11.011

Shankman, S.A., Campbell, M.L., Klein, D.N., Leon, A.C., Arnow, B.A., Manber, R., Keller, M.B., Markowitz, J.C., Rothbaum, B.O., Thase, M.E., Kocsis, J.H., 2013. Dysfunctional attitudes as a moderator of pharmacotherapy and psychotherapy for chronic depression. J. Psychiatr. Res. 47, 113–121. https://doi.org/10.1016/j.jpsychires.2012.09.018

Smith, S.M., 2002. Fast robust automated brain extraction. Hum. Brain Mapp. 17, 143–155. https://doi.org/10.1002/hbm.10062

Smith, S.M., Jenkinson, M., Johansen-Berg, H., Rueckert, D., Nichols, T.E., Mackay, C.E., Watkins, K.E., Ciccarelli, O., Cader, M.Z., Matthews, P.M., Behrens, T.E.J., 2006. Tract-based spatial statistics: Voxelwise analysis of multi-subject diffusion data. NeuroImage 31, 1487–1505. https://doi.org/10.1016/j.neuroimage.2006.02.024

Smith, S.M., Jenkinson, M., Woolrich, M.W., Beckmann, C.F., Behrens, T.E.J., Johansen-Berg, H., Bannister, P.R., De Luca, M., Drobnjak, I., Flitney, D.E., Niazy, R.K., Saunders, J., Vickers, J., Zhang, Y., De Stefano, N., Brady, J.M., Matthews, P.M., 2004. Advances in functional and structural MR image analysis and implementation as FSL. Neuroimage 23, S208–S219. https://doi.org/10.1016/j.neuroimage.2004.07.051

Spinhoven, P., Klein, N., Kennis, M., Cramer, A.O.J., Siegle, G., Cuijpers, P., Ormel, J., Hollon, S.D., Bockting, C.L., 2018. The effects of cognitive-behavior therapy for depression on repetitive negative thinking: A meta-analysis. Behav. Res. Ther. 106, 71–85. https://doi.org/10.1016/j.brat.2018.04.002

Teicher, M.H., Samson, J.A., 2013. Childhood maltreatment and psychopathology: A case for ecophenotypic variants as clinically and neurobiologically distinct subtypes. Am. J. Psychiatry 170, 1114–1133. https://doi.org/10.1176/appi.ajp.2013.12070957

Teicher, M.H., Samson, J.A., Anderson, C.M., Ohashi, K., 2016. The effects of childhood maltreatment on brain structure, function and connectivity. Nat. Rev. Neurosci. 17, 652–666. https://doi.org/10.1038/nrn.2016.111

Tiego, J., Martin, E.A., DeYoung, C.G., Hagan, K., Cooper, S.E., Pasion, R., Satchell, L., Shackman, A.J., Bellgrove, M.A., Fornito, A., Abend, R., Goulter, N., Eaton, N.R., Kaczkurkin, A.N., Nusslock, R., 2023. Precision behavioral phenotyping as a strategy for uncovering the biological correlates of psychopathology. Nat. Ment. Health 1, 304–315. https://doi.org/10.1038/s44220-023-00057-5

Tokuda, T., Yoshimoto, J., Shimizu, Y., Okada, G., Takamura, M., Okamoto, Y., Yamawaki, S., Doya, K., 2018. Identification of depression subtypes and relevant brain regions using a data-driven approach. Sci. Rep. 8, 14082. https://doi.org/10.1038/s41598-018-32521-z

Tozzi, L., Zhang, X., Pines, A., Olmsted, A.M., Zhai, E.S., Anene, E.T., Chesnut, M., Holt-Gosselin, B., Chang, S., Stetz, P.C., Ramirez, C.A., Hack, L.M., Korgaonkar, M.S., Wintermark, M., Gotlib, I.H., Ma, J., Williams, L.M., 2024. Personalized brain circuit scores identify clinically distinct biotypes in depression and anxiety. Nat. Med. 30, 2076–2087. https://doi.org/10.1038/s41591-024-03057-9

Vai, B., Parenti, L., Bollettini, I., Cara, C., Verga, C., Melloni, E., Mazza, E., Poletti, S., Colombo, C., Benedetti, F., 2020. Predicting differential diagnosis between bipolar and unipolar depression with multiple kernel learning on multimodal structural neuroimaging. Eur. Neuropsychopharmacol. 34, 28–38. https://doi.org/10.1016/j.euroneuro.2020.03.008

van der Kolk, B.A., 2003. The neurobiology of childhood trauma and abuse. Child Adolesc. Psychiatr. Clin. 12, 293–317. https://doi.org/10.1016/S1056-4993(03)00003-8

Waller, L., Erk, S., Pozzi, E., Toenders, Y.J., Haswell, C.C., Büttner, M., Thompson, P.M., Schmaal, L., Morey, R.A., Walter, H., Veer, I.M., 2022. ENIGMA HALFPIPE□: Interactive, reproducible, and efficient analysis for resting□state and task□based FMRI data. Hum. Brain Mapp. 43, 2727–2742. https://doi.org/10.1002/hbm.25829

Wiles, N., Thomas, L., Abel, A., Ridgway, N., Turner, N., Campbell, J., Garland, A., Hollinghurst, S., Jerrom, B., Kessler, D., Kuyken, W., Morrison, J., Turner, K., Williams, C., Peters, T., Lewis, G., 2013. Cognitive behavioural therapy as an adjunct to pharmacotherapy for primary care based patients with treatment resistant depression: results of the CoBalT randomised controlled trial. The Lancet 381, 375–384. https://doi.org/10.1016/S0140-6736(12)61552-9

Williams, L.M., 2017. Defining biotypes for depression and anxiety based on large-scale circuit dysfunction: a theoretical review of the evidence and future directions for clinical translation. Depress. Anxiety

34, 9–24. https://doi.org/10.1002/da.22556
Williams, L.M., 2016. Precision psychiatry: a neural circuit taxonomy for depression and anxiety. Lancet Psychiatry 3, 472–480. https://doi.org/10.1016/S2215-0366(15)00579-9
Woolrich, M.W., Jbabdi, S., Patenaude, B., Chappell, M., Makni, S., Behrens, T., Beckmann, C., Jenkinson, M., Smith, S.M., 2009. Bayesian analysis of neuroimaging data in FSL. Neuroimage 45, S173-86. https://doi.org/10.1016/j.neuroimage.2008.10.055
Xia, M., Womer, F.Y., Chang, M., Zhu, Y., Zhou, Q., Edmiston, E.K., Jiang, X., Wei, S., Duan, J., Xu, K., Tang, Y., He, Y., Wang, F., 2019. Shared and Distinct Functional Architectures of Brain Networks Across Psychiatric Disorders. Schizophr. Bull. 45, 450–463. https://doi.org/10.1093/schbul/sby046
Xie, C., Xiang, S., Shen, C., Peng, X., Kang, J., Li, Y., Cheng, W., He, S., Bobou, M., Broulidakis, M.J., van Noort, B.M., Zhang, Z., Robinson, L., Vaidya, N., Winterer, J., Zhang, Y., King, S., Banaschewski, T., Barker, G.J., Bokde, A.L.W., Bromberg, U., Büchel, C., Flor, H., Grigis, A., Garavan, H., Gowland, P., Heinz, A., Ittermann, B., Lemaître, H., Martinot, J.-L., Martinot, M.-L.P., Nees, F., Orfanos, D.P., Paus, T., Poustka, L., Fröhner, J.H., Schmidt, U., Sinclair, J., Smolka, M.N., Stringaris, A., Walter, H., Whelan, R., Desrivières, S., Sahakian, B.J., Robbins, T.W., Schumann, G., Jia, T., Feng, J., 2023. A shared neural basis underlying psychiatric comorbidity. Nat. Med. 29, 1232–1242. https://doi.org/10.1038/s41591-023-02317-4
Yan, L., Kraaijenvanger, E.J., Wennekers, R., Müller, V.I., Eickhoff, S.B., Fernández, G., Holz, N.E., Kohn, N., 2025. The effects of childhood adversity: Two specific neural patterns. Neurosci. Biobehav. Rev. 174, 106176. https://doi.org/10.1016/j.neubiorev.2025.106176
Zang, Y., Jiang, T., Lu, Y., He, Y., Tian, L., 2004. Regional homogeneity approach to fMRI data analysis. Neuroimage 22, 394–400.
Zhou, Y., Arend, J., Mufson, L., Gunlicks-Stoessel, M., 2021. Change in dysfunctional attitudes and attachment in interpersonal psychotherapy for depressed adolescents. Psychother. Res. J. Soc. Psychother. Res. 31, 258–266. https://doi.org/10.1080/10503307.2020.1756513
Zou, Q.-H., Zhu, C.-Z., Yang, Y., Zuo, X.-N., Long, X.-Y., Cao, Q.-J., Wang, Y.-F., Zang, Y.-F., 2008. An improved approach to detection of amplitude of low-frequency fluctuation (ALFF) for resting-state fMRI: fractional ALFF. J. Neurosci. Methods 172, 137–141.

Table 1. Descriptive statistics of the whole sample

Variable	HC (N=138)	MDD (N=135)	BD (N=209)	F / χ2	p	pFDR	Post-hoc
Age	30.75±10.6	49.39±9.95	47.39±10.6	139.09	<0.001	<0.001*	MDD>HC BD>HC
Sex	77 F; 61 M	95 F; 40 M	133 F; 76 M	6.26	0.04	0.06	
Scanner	0 Gyroscan; 138 Igenia	48 Gyroscan; 87 Igenia	144 Gyroscan; 65 Igenia	166.07	<0.001	<0.001*	
No. of episodes	/	5.24±5.58	12.61±12.96	38.92	<0.001	<0.001*	BD>MDD
Age at onset	/	32.63±11.39	29.21±10.05	8.57	<0.001	0.01*	MDD>BD
Duration of illness (years)	/	16.76±10.52	18.18±10.96	1.42	0.23	0.26	
Years of education	16.51±3.04	12.86±3.9	11.88±3.78	69.82	<0.001	<0.001*	HC>MDD HC>BD MDD>BD
Pharmacological load	/	4.75±2.29	4.5±2.17	1.05	0.31	0.32	
HDRS-21 total score	/	22.48±6.99	22.43±4.85	0.01	0.93	0.93	
CTQ physical abuse[a]	5.62±1.58	6.55±4.37	5.96±2.07	2.64	0.07	0.09	
CTQ emotional abuse[a]	8.04±3.59	8.99±4.24	8.11±3.5	2.08	0.13	0.15	
CTQ sexual abuse[a]	5.06±0.78	6.04±2.96	5.63±1.88	5.61	<0.001	0.01*	MDD>HC BD>HC
CTQ physical neglect[a]	6.58±2.74	7.7±3.36	6.76±2.46	4.62	0.01	0.02*	MDD>HC MDD>BD
CTQ emotional neglect[a]	11.1±4.56	12.93±4.98	12.43±4.9	3.90	0.02	0.03*	MDD>HC MDD>BD
CTQ total score[a]	36.77±10.07	43.39±13.09	40.85±14.59	6.82	<0.001	<0.001*	MDD>HC BD>HC
CQ emotional impact[b]	3.04±3.17	4.17±2.61	4.18±3.02	3.06	0.05	0.06	
CQ attribution of causality[b]	3.5±2.2	4.93±2.34	5.5±2.57	12.08	<0.001	<0.001*	MDD>HC BD>HC
CQ generalization across time[b]	2.74±1.83	4.21±2.89	4.64±3.03	8.23	<0.001	<0.001*	MDD>HC BD>HC
CQ generalizzation	3.76±2.51	6.15±2.9	6.26±3.05	14.43	<0.001	<0.001*	MDD>HC BD>HC

across events[b]							
CQ perceived uncontrollability[b]	2.68±2.05	3.54±2.63	4.1±2.76	5.38	0.01	0.01*	BD>HC
CQ total score[b]	14.26±7.71	23±10.4	24.64±11.2	18.33	<0.001	<0.001*	MDD>HC BD>HC

Results are reported as mean ± standard deviation for continuous variables, whereas frequencies are reported for categorical variables. Abbreviations: HC, Healthy Controls; MDD, Major Depressive Disorder; BD, Bipolar Disorder; HDRS-21, Hamilton Depression Rating Scale – 21 items; CTQ, Childhood Trauma Questionnaire; CQ, Cognition Questionnaire. [a]subsample of N=327 (MDD=106; BD=123; HC=98); [b]subsample of N=258 (MDD=87; BD=121; HC=50); *FDR-corrected q<0.05.

Table 2. Clustering models' performance

Model	Algorithms	Clusters	Stability (error)	Acc	Sil	DB	q
FC	Kmeans + SVM	2	0.15(0.02)	84.8	0.29(2)	1.24(2)	<0.001*
GM	Kmeans + SVM	2	0.17(0.01)	83.2	0.14(2)	2.14(2)	<0.001*
CT	Kmeans + SVM	2	0.18(0.02)	81.9	0.27(2)	1.51(2)	<0.001*
RD	Kmeans + SVM	2	0.20(0.02)	80.1	0.17(2)	1.90(2)	0.002*
FA	Kmeans + SVM	2	0.21(0.01)	79.2	0.20(2)	1.73(2)	<0.001*
AD	Kmeans + SVM	2	0.21(0.01)	78.8	0.15(2)	2.11(2)	<0.001*
MD	Kmeans + SVM	2	0.24(0.02)	76.5	0.20(2)	1.84(2)	0.04*
Multimodal	Multiview + SVM	2	0.27(0.04)	73.4	0.49(2)	0.76(2)	0.002*
ReHo	Kmeans + SVM	2	0.59(0.04)	40.9	0.07(2)	3.21(3)	0.044*
fALFF	Kmeans + SVM	3	0.67(0.03)	31.6	0.10(2)	3.04(5)	0.852

For each feature, number of clusters, normalized stability measures, and accuracies (in percentage) are reported. For comparison, the number of clusters identified based on internal measures (i.e., Silhouette and Davies-Bouldin scores) are reported in brackets. Models are sorted based on normalized stability measures, where lower values indicate a more stable clustering solution. FDR-corrected q-values obtained from 10,000 Monte-Carlo simulations are reported. Abbreviations: Acc, accuracy; Sil, Silhouette score; DB, Davies-Bouldin score; FC, functional connectivity; GM, grey matter; CT, cortical thickness; RD, radial diffusivity; FA, fractional anisotropy; AD, axial diffusivity; MD, mean diffusivity; ReHo, regional homogeneity; fALFF, fractional amplitude of low frequency fluctuations; SVM, support vector machine. *FDR-corrected q<0.05.

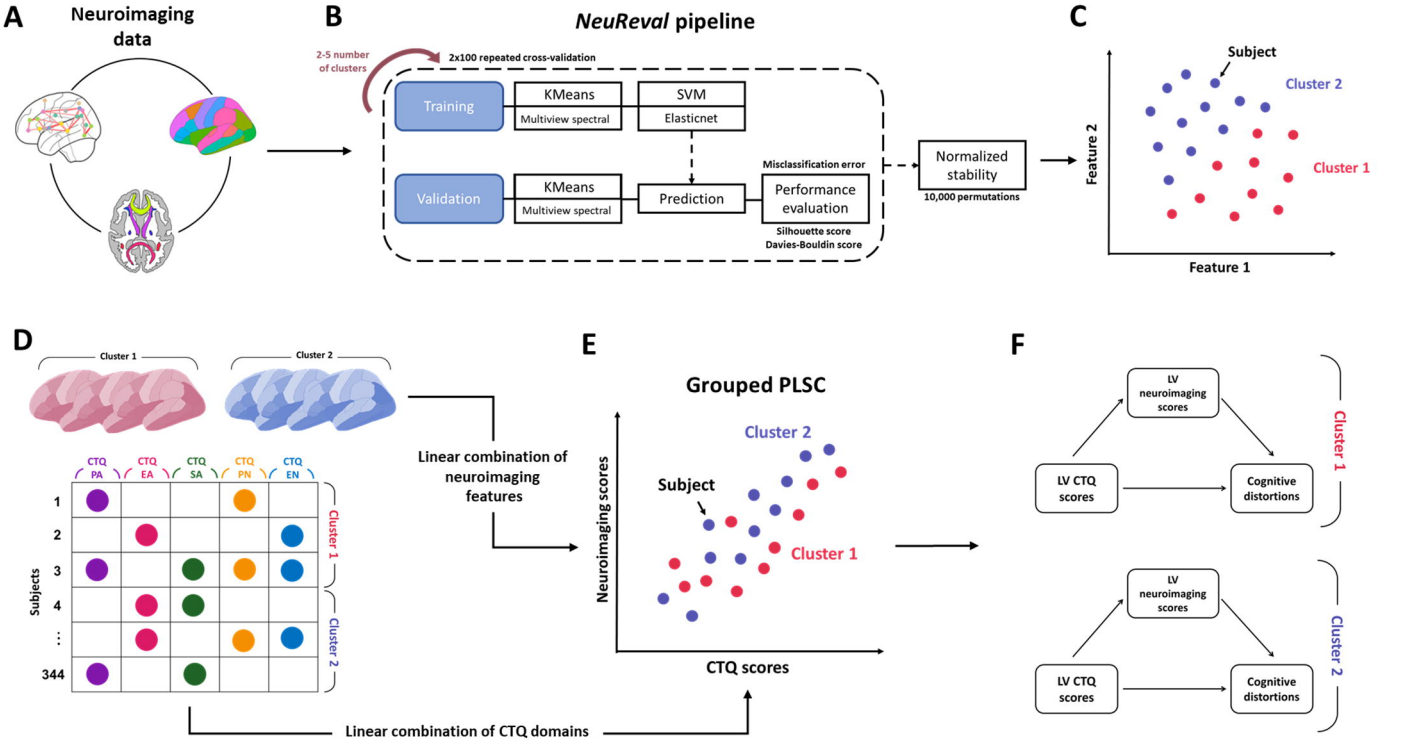
A
Neuroimaging data
B
NeuReval pipeline
2-5 number of clusters
2x100 repeated cross-validation
Training
KMeans
Multiview spectral
SVM
Elasticnet
Validation
KMeans
Multiview spectral
Prediction
Misclassification error
Performance evaluation
Silhouette score
Davies-Bouldin score
Normalized stability
10,000 permutations
C
Subject
Cluster 2
Cluster 1
Feature 2
Feature 1
D
Cluster 1
Cluster 2
CTQ PA
CTQ EA
CTQ SA
CTQ PN
CTQ EN
Subjects
1
2
3
4
⋮
344
Cluster 1
Cluster 2
Linear combination of neuroimaging features
Linear combination of CTQ domains
E
Grouped PLSC
Cluster 2
Subject
Cluster 1
Neuroimaging scores
CTQ scores
F
LV neuroimaging scores
LV CTQ scores
Cognitive distortions
Cluster 1
LV neuroimaging scores
LV CTQ scores
Cognitive distortions
Cluster 2

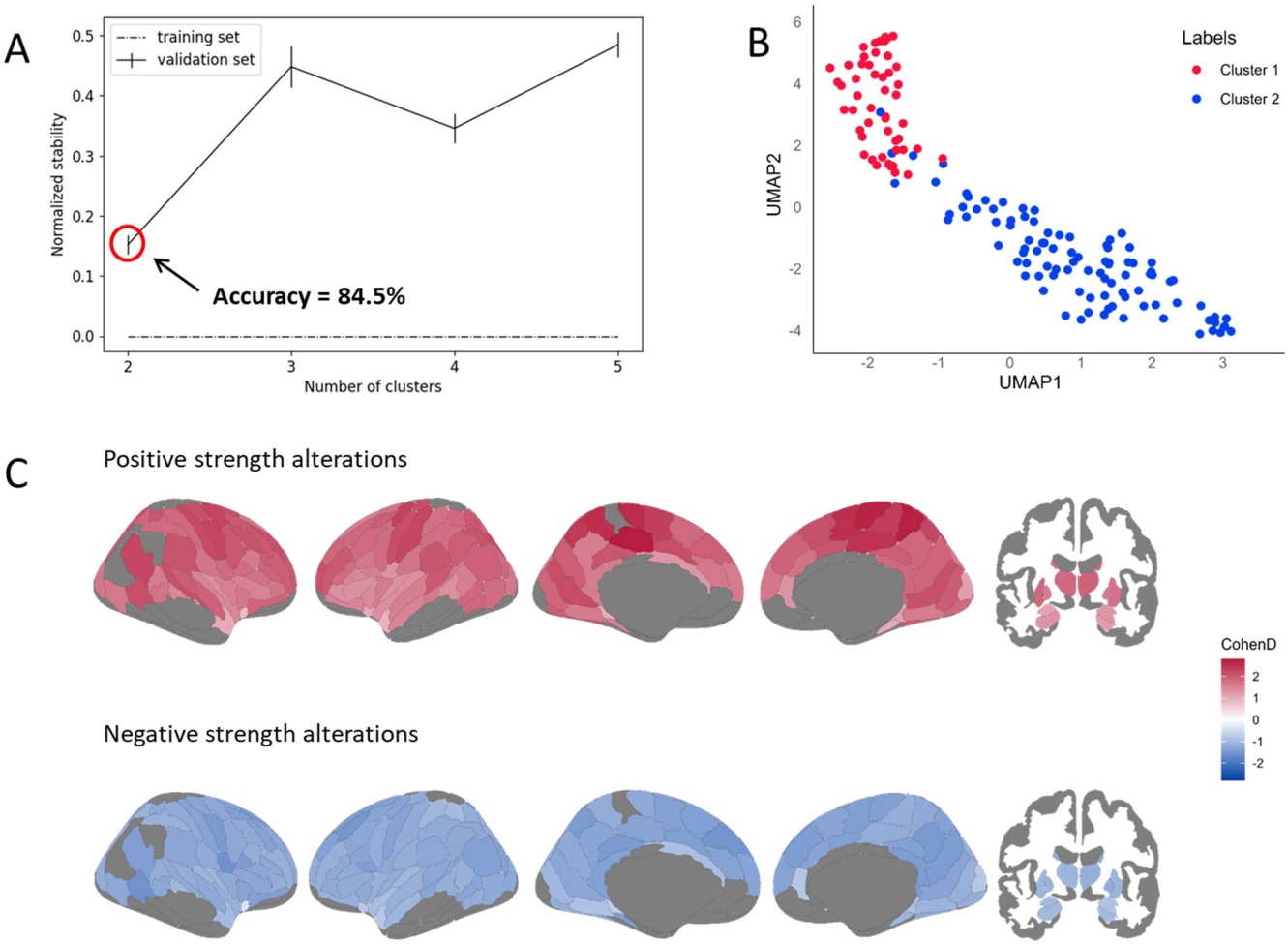
A
training set
validation set
Normalized stability
0.5
0.4
0.3
0.2
0.1
0.0
Accuracy = 84.5%
2
3
4
5
Number of clusters
B
Labels
Cluster 1
Cluster 2
UMAP2
6
4
2
0
-2
-4
UMAP1
-2
-1
0
1
2
3
C
Positive strength alterations
Negative strength alterations
CohenD
2
1
0
-1
-2

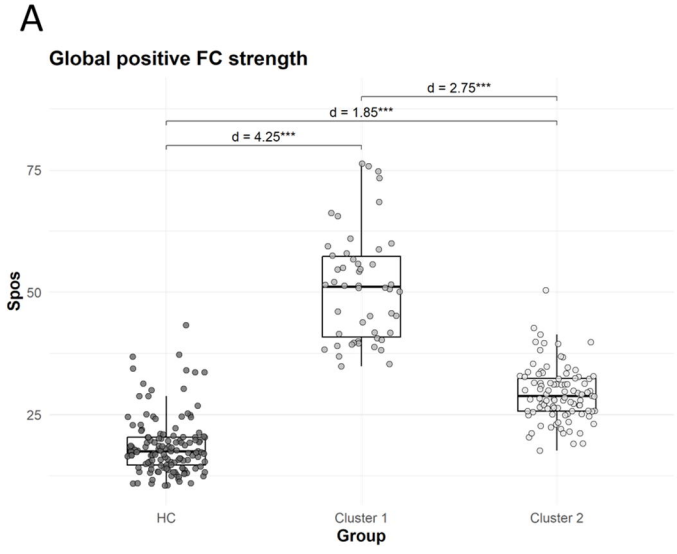
A
Global positive FC strength
d = 2.75***
d = 1.85***
d = 4.25***
75
50
25
Spos
HC
Cluster 1
Cluster 2
Group

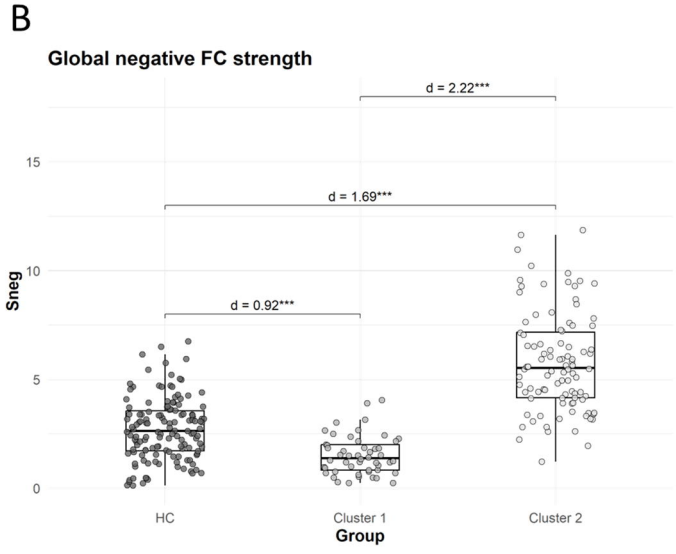
B
Global negative FC strength
d = 2.22***
d = 1.69***
d = 0.92***
15
10
5
0
Sneg
HC
Cluster 1
Cluster 2
Group

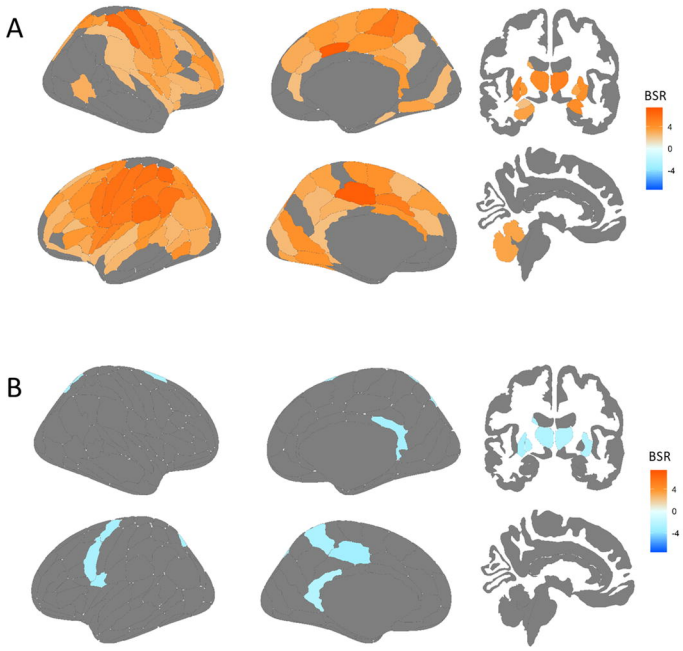
A
BSR
4
0
-4
B
BSR
4
0
-4

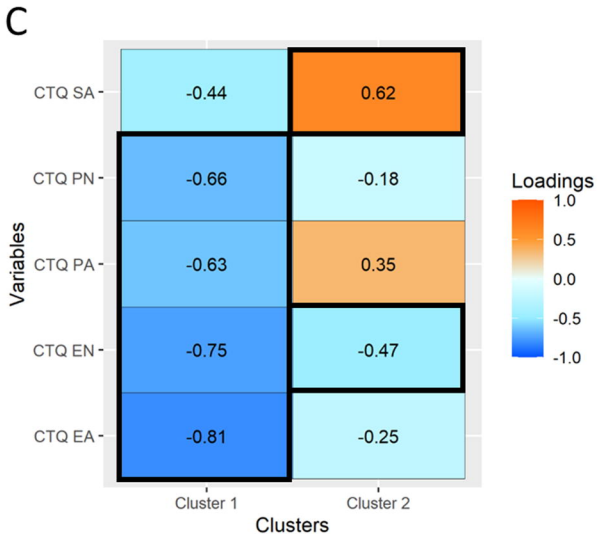
C
CTQ SA
CTQ PN
CTQ PA
CTQ EN
CTQ EA
Variables
-0.44
0.62
-0.66
-0.18
-0.63
0.35
-0.75
-0.47
-0.81
-0.25
Cluster 1
Cluster 2
Clusters
Loadings
1.0
0.5
0.0
-0.5
-1.0

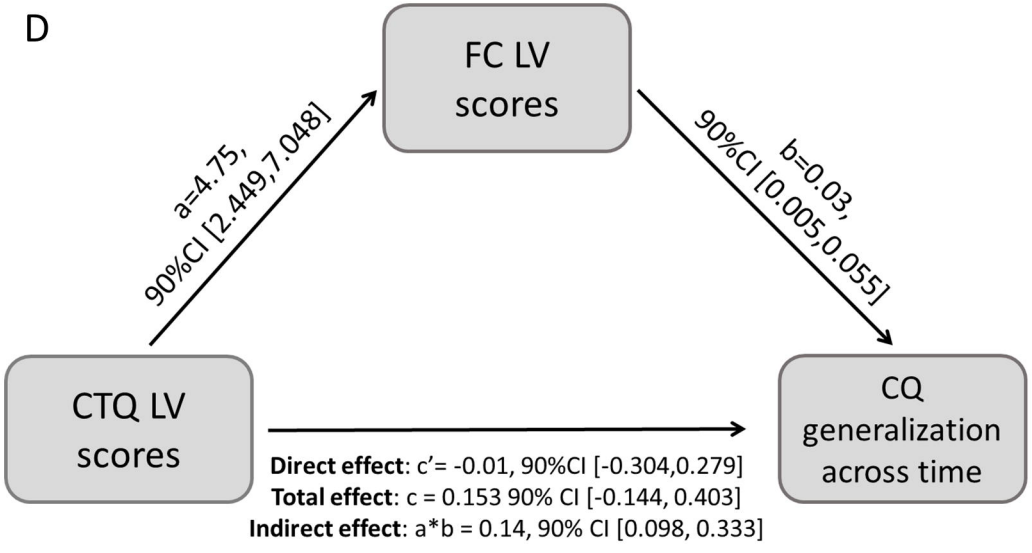
D
FC LV scores
a=4.75,
90%CI [2.449,7.048]
b=0.03,
90%CI [0.005,0.055]
CTQ LV scores
CQ generalization across time
Direct effect: c'= -0.01, 90%CI [-0.304,0.279]
Total effect: c = 0.153 90% CI [-0.144, 0.403]
Indirect effect: a*b = 0.14, 90% CI [0.098, 0.333]